Journal of Controlled Release 137 (2009) 224–233

Contents lists available at ScienceDirect

Journal of Controlled Release

journal homepage: www.elsevier.com/locate/jconrel

Tailored drug release from biodegradable stent coatings based on hybrid polyurethanes

Qiongyu Guo [a,b], Pamela T. Knight [a,b], Patrick T. Mather [b,c,*]

[a] Department of Macromolecular Science and Engineering, Case Western Reserve University, 2100 Adelbert Road, Cleveland, OH 44106, United States
[b] Syracuse Biomaterials Institute, Syracuse University, Syracuse, NY 13244, United States
[c] Department of Biomedical and Chemical Engineering, Syracuse University, Syracuse, NY 13244, United States

ARTICLE INFO

Article history:
Received 28 October 2008
Accepted 10 April 2009
Available online 17 April 2009

Keywords:
POSS
Biodegradable polymer
Drug delivery
Drug-eluting stents

ABSTRACT

Highly adjustable and precisely controllable drug release from a biodegradable stent coating was achieved using a unique family of nanostructured hybrid polyurethanes. These polyurethanes are polyhedral oligosilsesquioxane thermoplastic polyurethanes (POSS TPUs) featuring alternating multiblock structures formed by nanostructured hard segments of POSS and biodegradable soft segments of a polylactide/caprolactone copolymer (P(DLLA-co-CL)) incorporating polyethylene glycol (PEG) covalently. POSS aggregated to form crystals serving as physical crosslinks on the nanometer scale, while the soft segments were designed carefully to modulate the drug release rate from the POSS TPU stent coatings in PBS buffer solution, with 90% of the drug releasing from within half a day to about 90 days. In order to interpret the underlying drug release mechanisms, an approximation model capable of describing the entire drug release process was developed. This model is based on Fickian diffusional transport, but also takes into account the polymer degradation and/or swelling of the coating, depending on the dominance of the degradation/swelling behavior compared to that of the diffusion characteristics. A general methodology was utilized for statistically fitting the drug release curves from the POSS TPU stent coatings using the model. We observed that the fitted initial drug release diffusion coefficient covered more than three orders of magnitude, depending on the polymer glass transition temperature (T_g), according to a modified Williams–Landel–Ferry (WLF) equation. In addition, two additional rate constants describing the impact of degradation and swelling on drug elution were determined and found to be consistent with independent measurements. Our results clearly show that the studied hybrid polyurethane family allows a drug release rate that is effectively manipulated through variation in polymer T_g, degradation rate, and thickness increment rate.

Published by Elsevier B.V.

1. Introduction

Drug-eluting stents (DES) were widely adopted in percutaneous coronary intervention treatment shortly after their introduction into the US market in 2003 [1,2], and have been implanted in almost 3 million Americans [3]. As of the end of 2007, the two primarily used DES were the polymer-coated Taxus® Paclitaxel-Eluting Stent (Boston Scientific, Natick, MA, USA) and the polymer-coated Cypher® Sirolimus-Eluting Stent (Cordis, Johnson and Johnson, Miami Lakes, FL, USA). Their release of paclitaxel (PTx) or sirolimus, respectively, has markedly benefited patients based on clinical outcomes, as compared to bare metal stents [4,5]. An opportunity exists to determine if a biodegradable polymer would positively impact the long term safety profile of drug-eluting stents [6–8]. Recently, efforts have been made to utilize biodegradable polymer coatings on stents to achieve coatings that degrade concurrently with controlled drug delivery [9–13]. The clinical trial by Wessely et al. using a polylactide-derived polyester as the biodegradable stent coating indicated that the drug release kinetics of paclitaxel played an important role in the DES performance [14]. Lao et al. evaluated the influence of the paclitaxel release kinetics on the smooth muscle cell proliferation in their short-term *in vitro* cell studies [15]. In order to adjust the drug release kinetics, Westedt et al. investigated poly(vinyl alcohol)-graft-poly(lactide-co-glycolide) (PVA-g-PLGA), using grafted PLGA with different chain lengths, as the biodegradable stent coating [16]. Hanefeld et al. employed poly(d,l-lactide)-poly(ethylene oxide)-poly(d,l-lactide) triblock copolymers as a stent coating material, but observed burst release of paclitaxel regardless of the copolymer composition [17]. Apart from drug release behavior, good mechanical properties of the stent coating are also required in order to maintain coating integrity on the stent strut during stent expansion and deployment [16]. Very recent studies have examined arterial deposition of drug released

* Corresponding author. Syracuse Biomaterials Institute, Syracuse University, Syracuse, NY 13244, United States.
E-mail address: ptmather@syr.edu (P.T. Mather).

0168-3659/$ – see front matter. Published by Elsevier B.V.
doi:10.1016/j.jconrel.2009.04.016

from the drug-eluting stents as influenced by release kinetics [18], thrombus formation [19], and luminal flow patterns [20].

Recently, our group has designed a novel family of biodegradable nanostructured hybrid polymers to be used as paclitaxel-loaded stent coatings, called polyhedral oligosilsesquioxane thermoplastic polyurethanes (POSS TPUs), with enhanced mechanical properties [21,22]. These polyurethanes feature an alternating multiblock structure formed by covalent connection of nanostructured hard segments of POSS, and biodegradable soft segments of poly-d,l-lactide/caprolactone copolymer (P(DLLA-co-CL)) incorporating polyethylene glycol (PEG). POSS is a uniquely designed cage-like silsesquioxane monomer that aggregates to form crystals that act as physical crosslinks in the POSS TPUs on the nanometer scale, leading to significant improvements in polymer mechanical properties [23]. On the other hand, the P(DLLA-co-CL) soft segment of the POSS TPUs can be conveniently modified by altering the PEG length and comonomer ratio of LA:CL, effectively changing various polymer properties, including glass transition temperature (T_g), hydrophilicity, and degradability. The controlled variability of this family of polyurethanes facilitated their use as drug release templates for a systematic drug release kinetics investigation.

Various mathematical models have been reported in the literature to elucidate the underlying release mechanisms of drug delivery from thin films or coatings [24,25]. In the simplest case of purely diffusion-controlled drug release from a non-biodegradable and non-swellable polymer matrix, exact solutions exist, but in practice are too complex for practical use [26]. For the more complex drug delivery systems involving biodegradation, swelling, and/or bioerosion, a rigorous analytical solution has remained intractable, and so researchers have turned to numerical analysis. Such an approach, while allowing accurate data fitting, is unsatisfying due to an inability to explicitly explore relationships between the drug release kinetics and physicochemical properties of the polymer matrix that would facilitate polymer design. Consequently, simplified approximation equations are highly desirable for better understanding of the effects of polymer variables on the drug release kinetics. To date, most approximation equations are only applicable to either the early stage or late stage of drug release profiles [27,28]. Very few approximations have been derived to illustrate the entire drug release process — the two most commonly used are the Weibull equation [29,30] and the Etters approximation equation [31]. Unfortunately, both equations utilize parameters lacking a physical basis in the drug release context, hindering them from extensive usage in complicated drug delivery systems [32–34].

The purpose of this study was to determine the degree of controlled PTx release from the POSS TPU family and then interpret the underlying drug release mechanisms through the use of a simple approximation model capable of describing the entire drug release process. Seven POSS TPUs were selected with varying T_g, hydrophilicity, degradability, and molecular weight, but with the hard-to-soft segment feed ratio (mol-%) kept constant. The newly developed model takes into account all three important physical phenomena; namely, Fickian diffusional transport, polymer degradation, and swelling of the coating. Each of the parameters was defined with their own representative rate constant and corresponding representative time constant. As we will show, polymer degradation or swelling only impacted drug release when their associated rate constant was comparable to the initial diffusion rate constant. The model was used to fit data from the *in vitro* drug release from POSS TPU stent coatings incorporating 5 wt.% paclitaxel. The fitted initial diffusion coefficient was quantitatively analyzed for its glass transition temperature dependence, and the other two fitted parameters, describing degradation and swelling, were compared with their experimental data. The drug release predictions using this model were also performed to compare the effect of each phenomenon on the drug release kinetics.

2. Materials and methods

2.1. Materials

Paclitaxel and Express® Coronary Stents (16 mm length × 1.5 mm diameter) were kindly provided by Boston Scientific Corporation (Natick, MA, USA). 7-epi-paclitaxel (97%) was purchased from InB: Hauser Pharmaceuticals Services Inc. (Denver, CO, USA) and used as received. Tetrahydrofuran (THF) and acetonitrile (HPLC grade) were purchased from Fisher. Buffer used for the degradation study was made from phosphate buffered saline (PBS) buffer packets (Sigma) containing 0.05% w/v Tween-20 surfactant and having a final pH of 7.4 and concentration of 0.01 M when combined with one liter of deionized water. Sodium azide (0.1 M solution) was purchased from Fluka, stored in the refrigerator (4 °C), and used as received. Glacial acetic acid, sodium dodecyl sulfate (SDS) (≥99%) and sodium phosphate monobasic (NaH_2PO_4, ≥99%) were purchased from Sigma-Aldrich and used as received.

2.2. POSS TPU preparation

Synthesis of the POSS TPUs was carried out as described earlier in a two-step fashion (Scheme 1) [22]. First, a α,ω-polymeric diol of P(DLLA-co-CL) (hereafter called polyol) was synthesized by the ring-opening polymerization of cyclic ester monomers in the presence of a prescribed concentration of initiating diol and small amount of organometallic catalyst. The purified polyol was then further reacted with a diisocyanate and POSS diol so that the final molar ratio of polyol to POSS was kept constant at 1:3. A more detailed synthetic procedure and methods of characterization can be found in the Supplementary data. The polymers used for stent coating are described in Table 1.

We designed a specific naming system to describe this family of POSS TPUs. It contains two parts starting with the synthesis information of the polyol followed by the information of the polyurethane. For instance, in the POSS TPU of $[P_{4k}LA_{100}CL_0]$-$[LP]_3$, the first part of $[P_{4k}LA_{100}CL_0]$ indicates that the POSS TPU contains the soft segment of P(DLLA-co-CL) synthesized using a PEG ${}_nM = 4$ kg/mol initiator and mole feed ratio of LA to CL repeat units of 100:0. The second part of $[LP]_3$ shows that the polyurethane synthesis step employed LDI and utilized a mole feed ratio of POSS to polyol of 3. Note that the first "P" in $[P_{4k}LA_{100}CL_0]$-$[LP]_3$ represents PEG, while the second "P" denotes POSS. Similarly, $[B\_LA_{97.5}CL_{2.5}]$-$[MP]_3$ consisted of a P(DLLA-co-CL) soft segment prepared using a 1,4-butanediol initiator instead of PEG, and mole feed ratio of LA to CL repeat units of 97.5:2.5. This POSS TPU utilized MDI with a mole feed ratio of POSS to polyol of 3. It should be noted that the mole feed ratio of LA monomer (3,6-dimethyl-1,4-dioxane-2,5-dione) to CL monomer (ε-caprolactone) was 95:5, instead of 97.5:2.5. This is due to the LA monomer having two LA repeat units, but the CL monomer having only one CL repeat unit.

2.3. POSS TPU film preparation and in vitro degradation

Films of all POSS TPUs were cast from THF solutions (10% w/v) using the following protocol. Dried polymer (1.5 g) was dissolved in THF (15 mL), then poured into a PTFE casting dish with a diameter of 10.5 cm, partially covered with a glass dish, and left in a chemical fume hood overnight to evaporate. The film (still in the dish) was then dried in a vacuum oven at 50–60 °C for at least 24 h. This process yielded clear, flexible films with a thickness of 0.3 mm. *In vitro* degradation for the POSS TPUs was performed by immersing cut samples (30–40 mg) with typical dimensions of 15 mm (length) × 5 mm (width) × 0.3 mm (thickness) in 20 mL of PBS buffer containing 0.05% w/v Tween-20 surfactant. The sample in buffer was held at 37 °C while being constantly agitated at 75 rpm in an incubator shaker (New Brunswick

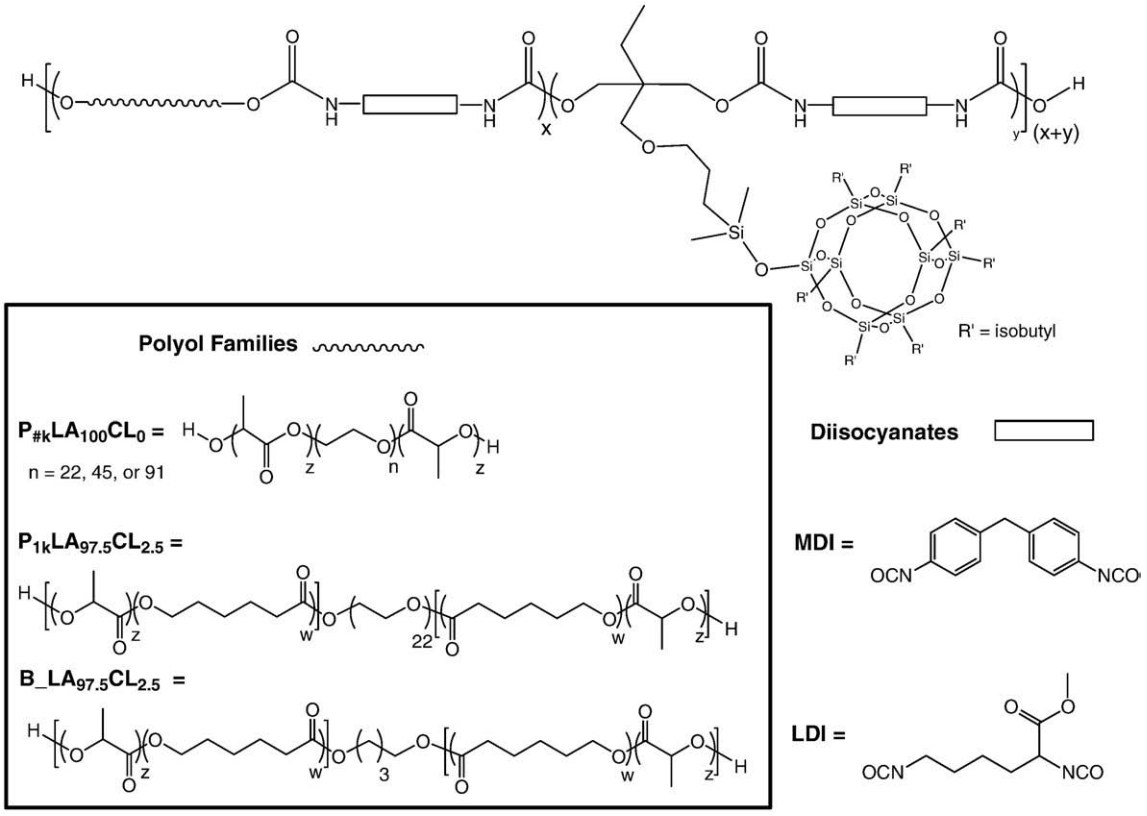

Scheme 1. General POSS TPU structure and the different polyols (〰) and diisocyanates (▭) used to create a variety of polyurethane compositions with different properties.

Scientific, Edison, NJ, USA). The buffer for each sample was decanted and replaced with fresh buffer every seven days. At predetermined time points, two samples were retrieved from the buffer, rinsed three times with deionized water, patted dry, and weighed. The samples were then dried for at least 5 days at room temperature under vacuum before being weighed again. The water uptake was determined by the ratio of the mass of the absorbed water to the mass of the degraded sample after drying under vacuum. The polymer mass remaining was calculated to be the ratio of the mass of the dried degraded sample to the mass of the original, non-degraded sample. Dried samples were also used to obtain the molecular weight by GPC.

2.4. Drug-loaded stent coating preparation and in vitro drug release

Paclitaxel-loaded POSS TPU coatings on Express® Coronary Stents were prepared for *in vitro* drug release tests using a proprietary coating process (micrographs in Supplementary data). The struts of each Express® Coronary Stent had a thickness of approximately 150 μm and width around 80 μm. Stents were coated in duplicate for each POSS TPU in Table 1 with a coating mass of 0.40 ± 0.04 mg consisting of 5 wt.% paclitaxel and 95 wt.% POSS TPU evenly blended together. Accordingly, the paclitaxel mass loaded in each stent was 20 ± 2 μg. Combining the coating mass with the stent surface area of 105.9 mm^2 and the POSS TPU density of 1.2 g/cm^3, the coating thickness was estimated to be 3.1 ± 0.3 μm, which has been verified to be around 3.5 μm using ion-milling/SEM, as detailed below in Section 2.6. The estimated coating thickness will be used in the calculations for drug release analyses.

In vitro drug release from the stent samples was undertaken in release media of PBS buffer with 0.05% w/v Tween-20 and 0.02% w/v sodium azide at pH = 7.4 kept in a 37 °C incubator shaker and agitated at 75 rpm. Each stent was placed in a 1.5 mL glass vial containing 1.5 mL of release medium. The release solution sampling time points were predetermined with the first week sampled at high frequency and the following weeks at lower frequency. According to the USP guideline, a sink condition can be maintained if the drug concentrations are kept at or below one third of the saturation solubility. We determined the solubility of amorphous paclitaxel to be 10 ± 1 μg/mL in the PBS buffer solution with Tween 20 at 37 °C and pH = 7.4. The sampling frequencies used were sufficiently high to maintain all the release solutions below the solubility limit and to keep 98% of the solutions in a sink condition (see Supplementary data for a histogram of paclitaxel concentrations measured). A preservative solution was prepared using 99.7% v/v acetonitrile and 0.3% v/v glacial acetic acid. At each time point, 0.4 mL of the release solution was collected and mixed with 0.2 mL of preservative solution to lower the pH so that the structure of paclitaxel could be stabilized [35]. The mixed working solution was stored at 4 °C until analyzed by high performance liquid chromatography (HPLC, Perkin Elmer, Waltham, MA, USA). The remaining release solution was removed, and new release medium of 1.5 mL was refilled into the same stent incubation vial. For each polymer coating studied, drug release experiments were run in

Table 1
Physicochemical properties of POSS TPUs.

POSS TPU	$\overline{M}_n$ (g/mol)/PDI	POSS ratio[a]	(CL:LA)%[a]	T_g (°C)	T_m (°C) (ΔH (J/g))
$[P_{4k}LA_{100}CL_0]$-$[LP]_3$	22,500/1.52	2.1	0	−1.0	131.0 (1.48)
$[P_{1k}LA_{90}CL_{10}]$-$[LP]_3$	55,700/1.40	3.0	16.0	17.3	129.6 (1.02)
$[P_{1k}LA_{97.5}CL_{2.5}]$-$[LP]_3$-1	23,400/2.89	2.0	2.7	24.7	115.0 (1.71)
$[P_{1k}LA_{97.5}CL_{2.5}]$-$[LP]_3$-2	79,100/1.52	2.7	2.7	24.6	110.8 (1.94)
$[P_{1k}LA_{100}CL_0]$-$[LP]_3$	28,100/1.59	1.8	0	31.4	119.2 (0.81)
$[P_{2k}LA_{100}CL_0]$-$[LP]_3$	24,400/1.48	2.1	0	31.8	114.0 (1.31)
$[B\_LA_{97.5}CL_{2.5}]$-$[MP]_3$	61,300/2.03	2.7	2.3	45.5	N/A[b]

[a] Actual ratio as determined by ^{1}H NMR.
[b] No melting observed by DSC (see Supplementary data for WAXD results).

duplicate with near-identical results observed and average values reported for each elution time point.

2.5. High performance liquid chromatography (HPLC)

The HPLC system (Perkin Elmer Series 200) included a vacuum degasser, an autosampler, a pump, a chromatography interface, and a UV/VIS detector set at 227 nm. The analytical column used was Waters® Symmetry C_{18} (4.6×75 mm, particle size 3.5 μm, pore size 100 Å). The mobile phase was 50:50 (v/v) HPLC grade water — HPLC grade acetonitrile with 20 mM SDS and NaH_2PO_4. The flow rate was set at 1 mL/min and total run time of the HPLC analysis was 8 min. Both paclitaxel and 7-epi-paclitaxel were observed in the HPLC chromatogram of the release solution. 7-epi-paclitaxel is the epimer of paclitaxel, the major degradation product of paclitaxel in the culture media at pH = 7.4 (Scheme 2) [36,37]. The retention times of paclitaxel and 7-epi-paclitaxel were 3.7 min and 6.2 min, respectively. Their calibration curves of the area-under-the-curve (AUC) vs. concentration were determined using four standard solutions with concentration of 0.0 μg/mL, 0.2 μg/mL, 1.0 μg/mL and 5.0 μg/mL to reveal linear relationships ($R^2 = 0.9999$). The ratio of calibration slopes for paclitaxel (α_p) to that for 7-epi-paclitaxel (α_e), α_p/α_e, was determined to be 1.098, which is close to the previously reported data [38]. The epimerization of paclitaxel to 7-epi-paclitaxel increased with the time required for complete drug release (Supplementary data). For the present study, we assumed no difference of the drug release kinetics between paclitaxel and 7-epi-paclitaxel and treated both drugs the same in the drug release calculations, unless otherwise specified. Thus, the fractional drug release was calculated by normalizing the sum of the released mass of both paclitaxel and 7-epi-paclitaxel by the total released mass of both drugs.

2.6. Scanning electron microscopy (SEM)

The morphologies of the stent coatings were examined using scanning electron microscopy (SEM, Model xT Nova Nanolab 200 with a dual focused ion beam (FIB) system, FEI, Hillsboro, OR, USA) at an accelerating voltage of 5 kV after being coated with a 10 nm layer of Pd. Stent coating thicknesses were measured using ion-milling/SEM.

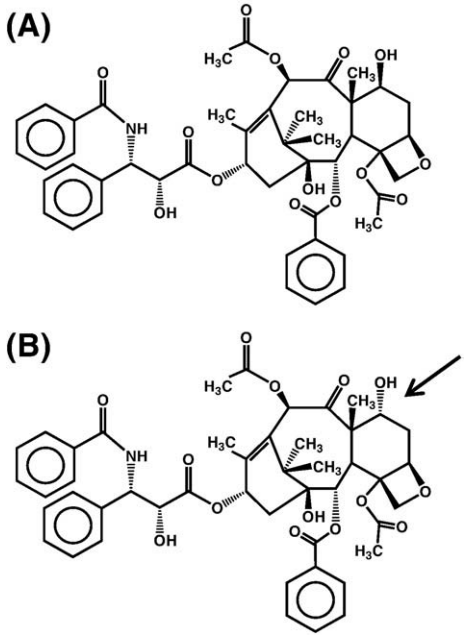

Scheme 2. Chemical structures of (A) paclitaxel, and (B) 7-epi-paclitaxel with an arrow pointing out the epimerized hydroxyl group.

Specifically, a layer of Pt of 15 μm×3 μm×1 μm on the coated stent was first deposited to protect the coating surface. Then a hole of 10 μm×10 μm×10 μm in the stent coating was milled using a low-energy Ga ion beam with the ion current of 30 pA and examined by the SEM.

3. Modeling

3.1. Drug release approximation equation and its simplified versions

Here, we formulate a simple approximation model for unidirectional (through-thickness, into buffer) drug release from biodegradable and swellable polymeric stent coatings based on Fick's second law (see Supplementary data for the equation derivation). Due to the degradation and swelling characteristics of the polymer matrix, the cumulative fractional drug release, $f(t)$, must incorporate a time-dependent diffusion coefficient, $D(t)$, and time-dependent thickness, $\delta(t)$,

$$f(t) \equiv \frac{m_t}{m_\infty} = 1 - \exp\left[-2\left(\frac{D(t)\cdot t}{\pi\delta(t)^2}\right)^{0.5}\right]. \quad (1)$$

Here, we assume the following time-dependency forms:

$$D(t) = D_0 \exp(kt) \quad (2)$$

$$\delta(t) = \delta_0(1 + \lambda t), \quad (3)$$

where $f(t)$ is defined as the ratio of the absolute cumulative mass of drug released at time t, m_t, to that at infinite time, m_∞. D_0 is the diffusion coefficient at $t = 0$, δ_0 is the coating thickness at $t = 0$, k denotes the polymer degradation rate constant, and λ represents the thickness increment rate constant. We consider "degradation" to include either plasticization, chain scission, or both, without differentiating the two. If we disregard the time-dependences of the diffusion coefficient and thickness, Eq. (1) approaches the well-accepted early-time approximation equation for drug release from a thin coating when $f(t) < 0.4$ [39]. Eq. (3) assumes the coating thickness increases linearly with time during the drug release process, as we observed in the family of POSS TPUs; however, other time-dependences could also be incorporated into the equation.

The time dependence of the diffusion coefficient in Eq. (2), as proposed by Charlier et al. [40], was based on two assumptions. First, we assume the polymer degradation follows first-order polymer chain cleavage kinetics as described by,

$$\overline{M}_n(t) = \overline{M}_n(0) \cdot \exp(-kt) \quad (4)$$

and, second, that the diffusion coefficient is proportional to the reciprocal of the polymer molecular weight,

$$D(t) = D_0 \times \left(\frac{\overline{M}_n(0)}{\overline{M}_n(t)}\right) \quad (5)$$

where $\overline{M}_n(t)$ is the number-average molecular weight of the polymer at time t, and $\overline{M}_n(0)$ is the initial number-average molecular weight of the polymer. It should be noted that, during polymer degradation, the diffusion coefficient may also be influenced by other factors, especially water absorption into polymer matrix and concomitant lowering of the polymer glass transition temperature. This could lead to a change of the magnitude of k in Eq. (2), compared to the k in Eq. (4).

Combining Eqs. (1)–(3) gives,

$$f(t) = 1 - \exp\left[-2\left(\frac{D_0 \exp(kt)\cdot t}{\pi\delta_0^2(1 + \lambda t)^2}\right)^{0.5}\right] \quad (6)$$

or more compactly,

$$f(t) = 1 - \exp\left\{-\frac{[(\beta t)\cdot \exp(kt)]^{0.5}}{(1+\lambda t)}\right\} \quad (7)$$

where β is the initial diffusion rate constant defined as,

$$\beta \equiv \frac{4D_0}{\pi\delta_0^2} \quad (8)$$

The three time constants corresponding to β, k and λ are defined as,

$$\tau_\beta \equiv \beta^{-1}, \tau_k \equiv k^{-1}, \tau_\lambda \equiv \lambda^{-1}$$

where τ_β, τ_k and τ_λ represent the initial diffusion time constant, degradation time constant and thickness increment time constant, respectively. Their independent measurement will require sufficient separation of their magnitudes.

Eq. (7) clearly incorporates the effects of degradation and swelling on drug release kinetics. It can be conveniently simplified to different drug release systems based on the relevance of each physical phenomenon. If the polymer carrier is hydrophobic and biodegradable, but does not swell significantly during the drug release process, i.e. $\tau_\lambda >> \tau_\beta$ and $\tau_\lambda >> \tau_k$, then λ can be set to 0. Eq. (7) then gives,

$$f(t) = 1 - \exp\left\{-[(\beta t)\cdot \exp(kt)]^{0.5}\right\} \quad (9)$$

If the polymer swells greatly, but does not degrade or degrades very slowly, i.e. $\tau_K >> \tau_\beta$ and $\tau_K >> \tau_\lambda$, then k can be set to 0 and Eq. (7) becomes,

$$f(t) = 1 - \exp\left[-\frac{(\beta t)^{0.5}}{(1+\lambda t)}\right] \quad (10)$$

Finally, if the drug release rate is large relative to insignificant swelling or degradation events; i.e., $\tau_\beta << \tau_k$ and $\tau_\beta << \tau_\lambda$, then both λ and k can be set to 0 and Eq. (7) is written as,

$$f(t) = 1 - \exp\left[-(\beta t)^{0.5}\right] \quad (11)$$

For our purposes, Eq. (7), together with the simplified equations Eqs. (9)–(11), will be utilized to fit the drug release curves from the POSS TPU stent coatings.

3.2. Statistical fitting

All statistical fittings were carried out using SigmaPlot 10.0 software. Specifically, the drug release profiles were fitted to Eq. (7) and simpler versions (Eqs. (9)–(11)), with the aim of identifying the simplest model that fits our data well. For this purpose, we used nonlinear regression with iterations of 100, step size of 100 and tolerance of 0.0001. As shown in Section 3.1, the new approximation equation (Eq. (7)) contained three fitting parameters (rate constants), while its derivative equations of Eqs. (9)–(11) had 2, 2, and 1 fitting parameters, respectively. Each equation under consideration was disregarded if unrealistic fitting parameters were reported, e.g. $\lambda < 0$, or gave a relative standard deviation higher than 100%. Equations were fit with the least amount of parameters that yielded the largest coefficient of determination, R^2. In this way the most suitable fitting equation was found for each drug release profile. In addition, linear regression was utilized to analyze the polymer molecular weight decrease with time, T_g effect on the initial diffusion coefficient, and swelling-induced thickening of the POSS TPU coatings on a stainless steel wire.

4. Results and discussion

4.1. POSS TPU selection criteria

Gaining quantitative understanding of drug release kinetics for our polymer family is inherently complicated due to the large combination of physical and chemical factors affecting the final results. In order to approach this problem systematically, we carefully designed a group of seven POSS TPUs comprising several variables which may play important roles in drug release kinetics (Table 1). These variables include T_g, hydrophilicity, and molecular weight. Specifically, we adjusted the PEG length and the comonomer ratio of LA:CL in the polyol soft segment of the polyurethane to modulate the POSS TPU T_g and hydrophilicity, but kept the POSS:polyol feed mole ratio constant to maintain the coating durability on the stents. All of the polyol segments used had a total molecular weight (including initiator) of 12 kg/mol, but the fraction of PEG incorporated through polyol initiation varied from zero for [B_$LA_{97.5}CL_{2.5}$]-$[MP]_3$, to 7 wt.% for [$P_{1k}LA_{100}CL_0$]-$[LP]_3$, [$P_{1k}LA_{97.5}CL_{2.5}$]-$[LP]_3$ and [$P_{1k}LA_{90}CL_{10}$]-$[LP]_3$, to 14 wt.% for [$P_{2k}LA_{100}CL_0$]-$[LP]_3$, to finally 28 wt.% for [$P_{4k}LA_{100}CL_0$]-$[LP]_3$. Increasing the PEG content in the polyols resulted in higher hydrophilicity of the POSS TPUs, as observed by an increase in equilibrium water-swelling. Specifically, the water uptake after one week of degradation was 2% for [B_$LA_{97.5}CL_{2.5}$]-$[MP]_3$, 4% for [$P_{1k}LA_{100}CL_0$]-$[LP]_3$, 21% for [$P_{2k}LA_{100}CL_0$]-$[LP]_3$, and 265% for [$P_{4k}LA_{100}CL_0$]-$[LP]_3$. On the other hand, both the PEG length and CL content strongly decreased the T_g of the POSS TPUs. As shown in Table 1, the T_g was lowered down from 46 °C for [B_$LA_{97.5}CL_{2.5}$]-$[MP]_3$, which contains no PEG, to −1 °C for [$P_{4k}LA_{100}CL_0$]-$[LP]_3$ with PEG $\overline{M}_n = 4$ kg/mol. Increasing CL content from 0% to 10% decreased T_g from 31 °C for [$P_{1k}LA_{100}CL_0$]-$[LP]_3$ to 17 °C for [$P_{1k}LA_{90}CL_{10}$]-$[LP]_3$. The large range of T_gs covered by this family of polymers allowed investigation into the T_g effect on drug release kinetics. In addition, two [$P_{1k}LA_{97.5}CL_{2.5}$]-$[LP]_3$ were synthesized to examine how the initial polymer molecular weight affected the drug release kinetics. Regardless of the varying compositions in POSS TPUs, we observed that the paclitaxel is amorphous and completely dissolved in the POSS TPU stent coatings. Therefore, the boundary conditions for the Fickian diffusion can be maintained during the drug release process from the paclitaxel-loaded POSS TPU stent coatings.

4.2. Model fitting

4.2.1. Drug release and glass transition temperature

In vitro drug release from POSS TPU stent coatings incorporating 5 wt.% paclitaxel was performed in PBS buffer solution containing Tween-20 and sodium azide and incubated at $T = 37$ °C. The coatings of the drug-loaded, polymer covered stents as prepared were smooth. After complete drug release, the coating morphology of these stents was still smooth and no pores were observed (Supplementary data for SEM images).

The drug release profiles of six POSS TPUs, as shown in Fig. 1, exhibited excellent reproducibility and were highly adjustable. The time required for 90% drug release, called t_{90}, was varied from half a day to about 90 days (Table 2). The drug release profile of [$P_{1k}LA_{97.5}CL_{2.5}$]-$[LP]_3$-2 is not shown in Fig. 1 due to near-perfect overlap with [$P_{1k}LA_{97.5}CL_{2.5}$]-$[LP]_3$-1. Using the fitting strategy mentioned in the statistical fitting section, all drug release profiles were well fitted by Eqs. (7), (9) or (11) (Fig. 1). Although valid in principle, Eq. (10) was not used for this polymer family, as will be explained below.

As shown in Table 2, the POSS TPUs could be divided into three subgroups depending on the suitable fitting equation used. The first subgroup contains four fast-releasing polymers, including [$P_{4k}LA_{100}CL_0$]-$[LP]_3$, [$P_{1k}LA_{90}CL_{10}$]-$[LP]_3$, [$P_{1k}LA_{97.5}CL_{2.5}$]-$[LP]_3$-1 and [$P_{1k}LA_{97.5}CL_{2.5}$]-$[LP]_3$-2, each fitted well by Eq. (11) with a single rate

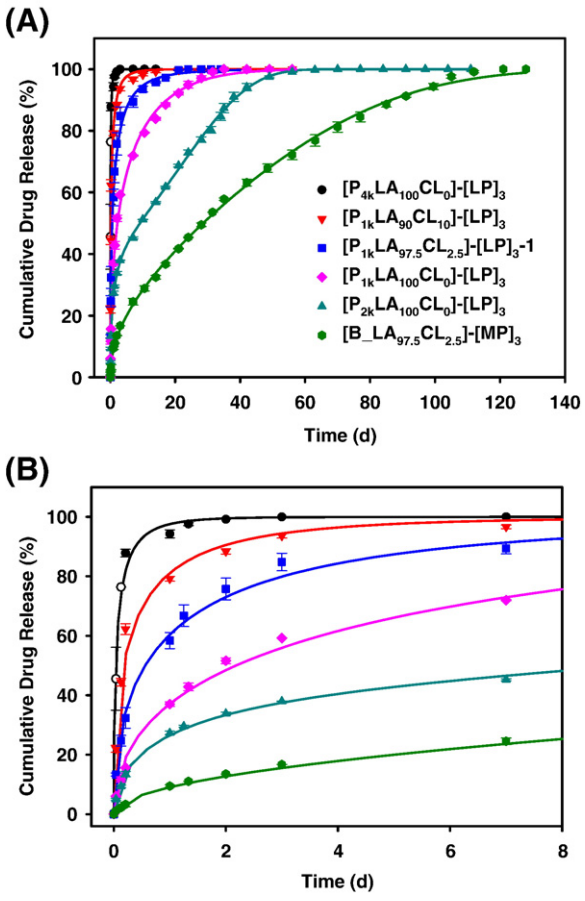

Fig. 1. Cumulative fractional drug release profiles and fit curves from POSS TPU stent coatings incorporated with 5 wt.% paclitaxel. Each point is the average of two experiments. (A) Full time period; (B) first week of drug release to reveal more detail at early times. The open symbols indicate several drug release solutions with concentration higher than the sink condition.

constant for diffusion, β. The second subgroup consists of two slow-releasing coatings of $[P_{1k}LA_{100}CL_0]$-$[LP]_3$ and $[B\_LA_{97.5}CL_{2.5}]$-$[MP]_3$ fitted well by Eq. (9) with two rate constants, β and k. The third subgroup contains only $[P_{2k}LA_{100}CL_0]$-$[LP]_3$ requiring all three rate constants of Eq. (7), β, k and λ, for a good fit. This is due to its degradation and swelling behavior. In general, when the POSS TPU initial diffusion time constant was much smaller than the degradation and thickness increment time constants, i.e. $\tau_\beta \ll \tau_k$ and $\tau_\beta \ll \tau_\lambda$, diffusional transport dominated the drug release, and thus Eq. (11) was applied for the first POSS TPU subgroup. Similarly, the degradation or thickness increment time constant was required in the fitting equation only when they were fast enough to affect the drug release kinetics, compared to the initial diffusion time constant. The fact that Eq. (10) was not suitable for any of the drug release profiles indicates that degradation plays a more important role in the drug release from POSS TPUs than swelling.

The initial drug release diffusion coefficients, D_0, were calculated using Eq. (8) from the fitting parameter β. They covered more than three orders of magnitudes from the highest value of 1.2×10^{-15} m^2/s found for $[P_{4k}LA_{100}CL_0]$-$[LP]_3$ to the lowest value of 8.0×10^{-19} m^2/s for $[B\_LA_{97.5}CL_{2.5}]$-$[MP]_3$, and clearly showed inverse dependence on the T_g values as measured from dried samples before degradation (Table 2). This trend of the initial drug release diffusion coefficient with polymer T_g was consistent with previous studies [41,42]. However, those studies modulated T_g by changing the polymer molecular weight, another factor capable of affecting the drug release kinetics. In this work, the T_g effect was separated from that of the polymer molecular weight effect on the initial diffusion coefficients by manipulating the glass transition temperature through the PEG length and CL content of the POSS TPUs while keeping the molecular weight approximately the same.

The relationship between the initial diffusion coefficient and the POSS TPU T_g before degradation could be described by a modified Williams–Landel–Ferry (WLF) equation as [43–45],

$$\log\left[\frac{D_0(T)}{D_0\left(T_g\right)}\right] = \frac{\xi C_{1g}\left(T - T_g\right)}{C_{2g} + T - T_g} \tag{12}$$

where T is the drug release temperature (kept constant at 37 °C in this work), and T_g was varied by polymer composition. C_{1g} and C_{2g} are the WLF parameters of the polymer matrix, and ξ represents a coupling parameter that characterizes the ratio of the critical molecular volume of the drug "jumping unit" to that of the polymer matrix "jumping unit", within the context of diffusion modeling in polymer media. The jumping units can be interpreted on the basis of Vrentas–Duda free-volume theory [46–48] as the discrete steps required for a single drug or polymer segments to achieve their diffusive motion. The T_g values of pure POSS TPUs were employed in this study because their T_gs did not change significantly upon the incorporation of 5 wt.% paclitaxel. The modified WLF equation is now well established in describing the diffusion of small rigid molecules in polymers above their glass transition temperature at low concentration. Typically, this equation has been used to investigate the temperature dependence of the diffusion coefficient for a certain polymer by adjusting the experimental diffusion temperature. To our knowledge, this is for the first extension of the modified WLF equation used for drug release where the polymer T_g varies, but where the drug release temperature is held constant at 37 °C, though in principle the two variations are the same. Assuming $D_0(T_g)$, C_{1g} and C_{2g} to be a constant for the POSS TPU family, though with variable T_g, Eq. (12) can be written as,

$$\log\left[D_0(T)\right] = \log\left[D_0\left(T_g\right)\right] + \xi C_{1g} \times \frac{\left(T - T_g\right)}{C_{2g} + T - T_g}, \tag{13}$$

suggesting a simple plotting scheme to test the equation and our assumptions, as we next describe.

As shown in Fig. 2, a linear relationship was observed for log $[D_0(T)]$ vs. $\frac{T - T_g}{C_{2g} + T - T_g}$ when using the universal WLF parameter

Table 2
Drug release characteristic parameters of fitting results for paclitaxel-loaded POSS TPU stent coatings[a].

POSS TPU	t_{90}(d)	β (d^{-1})	k (d^{-1})	λ (d^{-1})	τ_β (d)	τ_k (d)	τ_λ (d)	D_0 ($\times10^{-16}$ m^2/s)	R^2 (%)
$[P_{4k}LA_{100}CL_0]$-$[LP]_3$	0.5	13.7859	0	0	0.07	N/A	N/A	12.4283	99.0
$[P_{1k}LA_{90}CL_{10}]$-$[LP]_3$	2.3	2.7791	0	0	0.36	N/A	N/A	2.5054	99.1
$[P_{1k}LA_{97.5}CL_{2.5}]$-$[LP]_3$-1	7.4	0.8581	0	0	1.17	N/A	N/A	0.7736	99.6
$[P_{1k}LA_{97.5}CL_{2.5}]$-$[LP]_3$-2	10.4	0.5677	0	0	1.76	N/A	N/A	0.5118	99.6
$[P_{1k}LA_{100}CL_0]$-$[LP]_3$	18.6	0.2103	0.0213	0	4.76	46.95	N/A	0.1896	99.7
$[P_{2k}LA_{100}CL_0]$-$[LP]_3$	37.2	0.1131	0.1062	0.1513	8.84	9.42	6.61	0.1020	99.9
$[B\_LA_{97.5}CL_{2.5}]$-$[MP]_3$	88.2	0.0089	0.0223	0	112.36	44.84	N/A	0.0080	99.9

[a] See Supplementary data for the relative standard deviations (RSDs) of the fitting parameters.

value of C_{2g} as 51.6 °C [49], thus proving the validity of utilizing Eq. (12) in this work. In addition, ξC_{1g} was fitted to be 5.27 and ξ is calculated to be 0.30 when C_{1g} is set to the universal WLF parameter value of 17.44. The POSS TPU initial diffusion coefficient at T_g, $D_0(T_g)$, was determined to be 6.3×10^{-18} m^2/s, which is within the range reported previously for polymer glasses [43,44]. In other words, the POSS TPU diffusion coefficient at T_g before degradation is constant, despite the fact that these polymers feature different T_g, hydrophilicity, comonomer ratio, and molecular weight. Yet, if we look into the two $[P_{1k}LA_{97.5}CL_{2.5}]$-$[LP]_3$ chosen in Table 1, the initial diffusion coefficient of $[P_{1k}LA_{97.5}CL_{2.5}]$-$[LP]_3$-1 was slightly higher than that of $[P_{1k}LA_{97.5}CL_{2.5}]$-$[LP]_3$-2 probably due to its lower molecular weight. Nevertheless, the influence of molecular weight on initial diffusion coefficient at 37 °C was much smaller than that of the POSS TPU T_g. This indicates T_g plays a dominant role in the initial drug diffusion coefficient (i.e. D_0(37 °C)). In addition, although Eq. (12) typically applies to $T_g<T$ (=37 °C), the $[B\_LA_{97.5}CL_{2.5}]$-$[MP]_3$ with T_g of 46 °C still demonstrates a good linearity in Fig. 2 probably because its T_g was still in the vicinity of body temperature.

4.2.2. Impact of polymer degradation on drug release

One of the distinct physical phenomena embodied in our approximation model is polymer degradation. Comparison of each POSS TPU's degradation time constant, τ_k, with the time required for 90% drug release from the same polymer, t_{90}, allows discernment of the significance of the degradation in influencing the drug release kinetics. As shown in Table 2, both $[P_{2k}LA_{100}CL_0]$-$[LP]_3$ and $[B\_LA_{97.5}CL_{2.5}]$-$[MP]_3$ exhibit τ_k values significantly smaller than their t_{90} values, indicating that the degradation of these POSS TPUs impacts their drug release kinetics at an early stage of the drug release process. Interestingly, the t_{90} of $[B\_LA_{97.5}CL_{2.5}]$-$[MP]_3$ is even smaller than the initial diffusion time constant of this polymer, τ_β. The t_{90} value is much larger than the τ_β for polymers without degradation involved in the drug release process, which will be discussed later. Therefore, the ordering of time constants $\tau_k<t_{90}<\tau_\beta$ of $[B\_LA_{97.5}CL_{2.5}]$-$[MP]_3$ indicates that the degradation of this POSS TPU significantly increases its drug release rate.

We further examined the relationship of the drug release and the degradation of $[B\_LA_{97.5}CL_{2.5}]$-$[MP]_3$. As shown in Fig. 3A, the drug release profile of $[B\_LA_{97.5}CL_{2.5}]$-$[MP]_3$ was best fitted using Eq. (9), comprising the two time constants of τ_k and τ_β but setting the thickness increment time constant, τ_λ, to be infinity ($\lambda=0$). This can be explained by the insignificant water uptake of $[B\_LA_{97.5}CL_{2.5}]$-$[MP]_3$ during almost the entire drug release process, as demonstrated in Fig. 3B. On the other hand, a slight fitting deviation was observed in Fig. 3A at the very late stage of the drug release process, which is due to the transitions of both mass loss and water uptake shown in Fig. 3B. Although Fig. 3B exhibits the incubation time of this POSS TPU was as long as 112 days with no significant mass loss, its molecular weight begins to decrease instantaneously after incubation in buffer solution. Indeed, we observed that $\overline{M}_n(t)/\overline{M}_n(0)$ decreased exponentially with time, confirming the first-order polymer chain cleavage assumption in Eq. (4) (see Supplementary data for the molecular weight evolution). The degradation rate constant of k_{GPC} was determined to be 0.026 d^{-1}, very close to that fitted from the drug release profile, $k=0.022$ d^{-1}. This proves the feasibility of utilizing the degradation-controlled diffusion coefficient in the new approximation model.

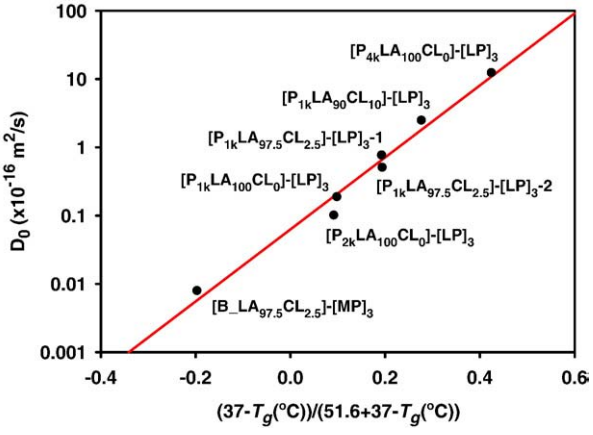

Fig. 2. POSS TPU initial diffusion coefficient D_0 vs. $(37-T_g(°C))/(51.6+37-T_g(°C))$. Note that the *y*-axis is a logarithmic scale.

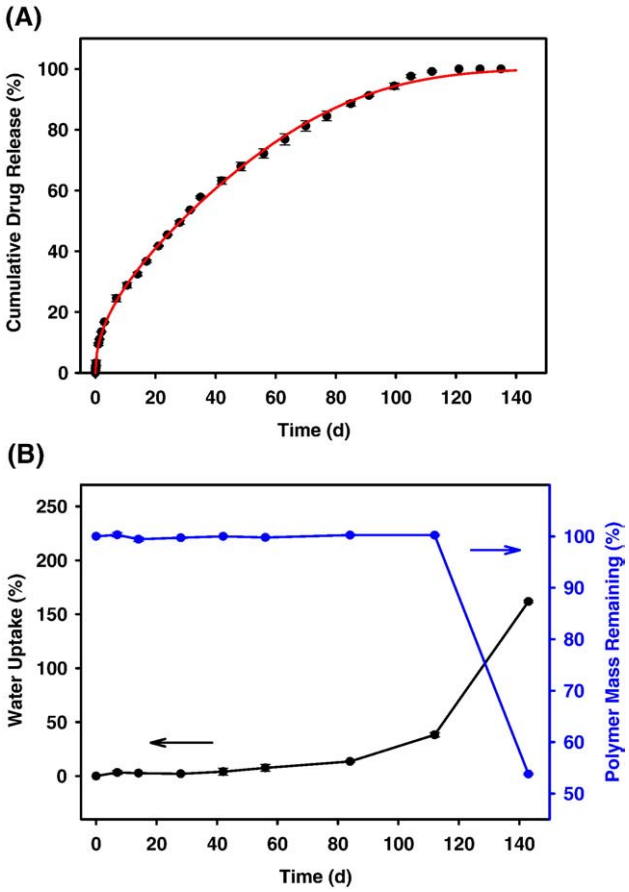

Fig. 3. (A) Cumulative fractional drug release profile of $[B\_LA_{97.5}CL_{2.5}]$-$[MP]_3$ stent coating incorporated with 5 wt.% paclitaxel fitted using Eq. (9) with R^2 of 99.91%, and (B) water uptake (left) and polymer mass remaining (right) evolution with time of the $[B\_LA_{97.5}CL_{2.5}]$-$[MP]_3$ film during *in vitro* degradation.

4.2.3. Impact of swelling on drug release

Another physical phenomenon considered in the new approximation model is the time-dependent thickness. As discussed above, the drug release profile of $[P_{2k}LA_{100}CL_0]$-$[LP]_3$ was best fitted using Eq. (7), consisting of both a time-dependent diffusion coefficient and time-dependent thickness. For this polymer, all three time constants were comparable, with the thickness increment time constant being the lowest (Table 2). This indicates significance of the swelling process of $[P_{2k}LA_{100}CL_0]$-$[LP]_3$ in its drug release kinetics. As shown in Fig. 4B, both water uptake and mass loss of $[P_{2k}LA_{100}CL_0]$-$[LP]_3$ changed almost linearly with time during the entire drug release process, the water uptake occurring faster than the mass loss, implying the linear swelling of this polymer, as adopted in Eq. (3). To further confirm this implication, we used a coated stainless steel wire to measure the thickness increment rate, λ_{direct}, of a $[P_{2k}LA_{100}CL_0]$-$[LP]_3$ coating over a two-week incubation in PBS buffer at 37 °C and pH=7.4. λ_{direct} was determined to be 0.10 d^{-1}, close to λ fitted from Eq. (7) (0.15 d^{-1})

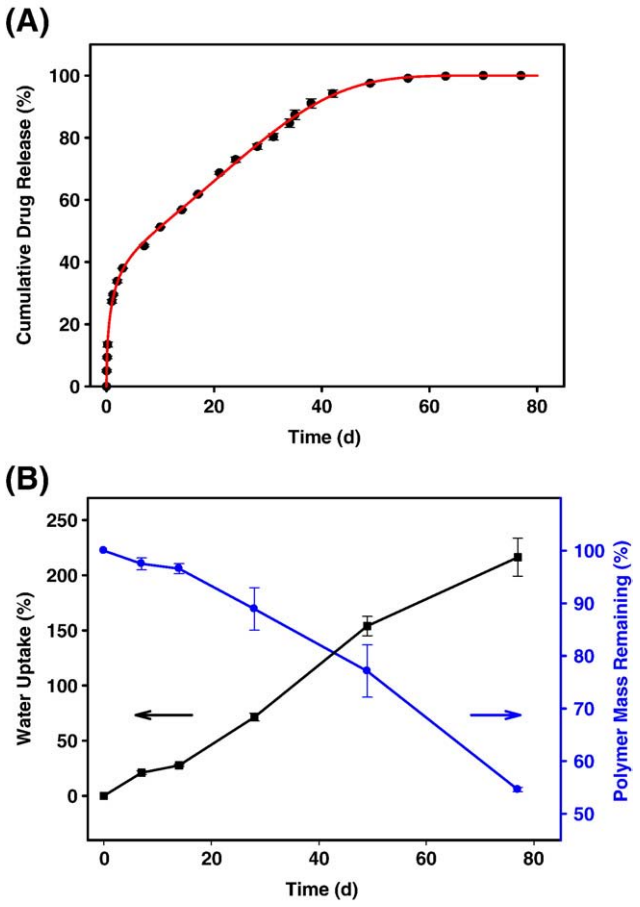

Fig. 4. (A) Cumulative fractional drug release profile of the $[P_{2k}LA_{100}CL_0]$-$[LP]_3$ stent coating incorporated with 5 wt.% paclitaxel fitted using Eq. (7) with R^2 of 99.93%, and (B) water uptake (left) and polymer mass remaining (right) evolution with time of the $[P_{2k}LA_{100}CL_0]$-$[LP]_3$ film during *in vitro* degradation.

(Supplementary data gives thickness increment rate determination). Therefore, the time-dependent thickness assumption also proves to be applicable to the new approximation model.

Interestingly, although $[P_{4k}LA_{100}CL_0]$-$[LP]_3$ was more hydrophilic and swelled more quickly than $[P_{2k}LA_{100}CL_0]$-$[LP]_3$, this polymer did not require the thickness increment time constant in its drug release fitting equation. This is most likely because $[P_{4k}LA_{100}CL_0]$-$[LP]_3$ took only half a day for 90% drug release, too short to be influenced by the swelling process. In contrast to $[P_{4k}LA_{100}CL_0]$-$[LP]_3$, $[P_{2k}LA_{100}CL_0]$-$[LP]_3$ required as long as 37 days for 90% drug release, leading to the overlapping of the swelling process with its drug release process. In addition, the mass loss witnessed for $[P_{2k}LA_{100}CL_0]$-$[LP]_3$ in Fig. 4B is apparently well accounted for by the rate constant of k by virtue of the high fitting quality of Fig. 4A.

4.2.4. Drug release predictions

Given the successful fitting of our drug elution data for the POSS TPU family with widely varying physical properties, we seek here to parametrically examine predictions for the effects of the glass transition, polymer degradation, and swelling on the drug release kinetics for polymers not yet synthesized. We recognize that the measurements of such physical parameters are simple compared to drug elution measurements, and so predictions along these lines are valuable. Fig. 5A shows predictions for T_g effect on the purely diffusion-controlled drug release without time-dependent polymer degradation or swelling. As such, it uses Eq. (11) with only one fitting parameter, β, calculated based on the fitting curve in Fig. 2 for the T_g values indicated. As expected, the drug release rate strongly depends on T_g, especially when T_g approaches or is higher than physiological temperature. In Fig. 5B, the polymer degradation effect is predicted using the same fitting equation found for $[B\_LA_{97.5}CL_{2.5}]$-$[MP]_3$ (Fig. 3A), but with systematic variation in degradation rate. As shown, the degradation efficiently alters the drug release rate, especially beyond the point of cumulative drug release higher than 20%. For instance, the time required for 90% drug release for $[B\_LA_{97.5}CL_{2.5}]$-$[MP]_3$ was measured to be 88 days, but it would be extended to more than one and a half years (i.e. 596 days) if $[B\_LA_{97.5}CL_{2.5}]$-$[MP]_3$ were non-degradable. Finally, Fig. 5C shows predictions for the swelling effect using the same fitting equation for

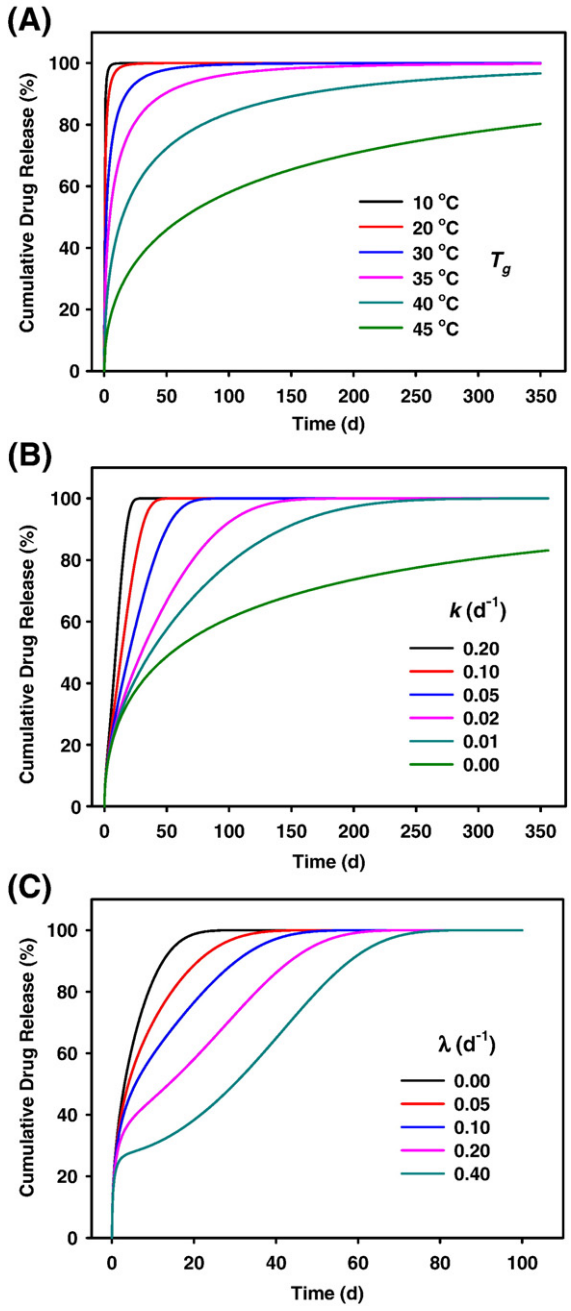

Fig. 5. Drug release predictions. (A) T_g effect prediction of purely diffusion-controlled drug release without time-dependent polymer degradation or swelling, predicted using Eq. (11). The initial diffusion coefficient is predicted from Fig. 2. (B) Degradation effect prediction using the same fitting equation of $[B\_LA_{97.5}CL_{2.5}]$-$[MP]_3$ in Fig. 3A, but with changes in degradation rate. (C) Thickness-increment effect prediction using the same equation of $[P_{2k}LA_{100}CL_0]$-$[LP]_3$ in Fig. 4A but with changes in thickness increment rate. The legends in (A), (B) and (C) were labeled from fastest to slowest drug release rates.

$[P_{2k}LA_{100}CL_0]$-$[LP]_3$ in Fig. 4A, but with systematic adjustment in thickness increment rate. Clearly, the swelling of the coating not only retards drug release for cumulative drug releases higher than 20%, but also changes the shape of the drug release curve. When the thickness increment rate constant is as high as 0.40 d^{-1}, the drug release rate is greatly slowed down at the cumulative drug release around 30%, leading to a period of drug release lag time of about ten days. This might explain why a drug release lag time sometimes happens after initial release burst in the biodegradable drug release systems reported previously [13]. Clearly, the drug release rate can be effectively lowered by increasing polymer T_g, reducing degradation rate, or enhancing the thickness increment rate.

5. Conclusions

Highly adjustable and precisely controllable drug release from paclitaxel-loaded stent coatings using seven biodegradable POSS TPUs with varying properties was achieved. A simple yet flexible approximation model was developed to fit and predict the entire drug release process from these POSS TPU coatings. Three distinct physical phenomena, i.e. Fickian diffusional transport, polymer degradation, and coating swelling, were all integrated in the model. Time constants characterizing each of the phenomena could be measured, revealing the extent of overlap in time among phenomena. Polymer degradation or coating swelling only influenced drug release kinetics when their time constants were close to or smaller than the initial diffusion time constant. Therefore, even within the same family of biodegradable and swellable polymers, drug release behavior could be divided by the model into purely diffusion-controlled drug release system, degradation-dominated drug release system, swelling-dominated release system, and degradation and swelling-governed drug release system, depending on the relative importance of each physical phenomenon. Yet, this model is not limited to biodegradable and swellable polymer system, but also applicable to non-degradable and/or non-swellable polymer. Although the approximation equation of Eq. (6) was derived assuming first-order polymer chain cleavage and linear polymer coating swelling, the time-dependences of the polymer degradation and coating thickness may be able to be modified to adapt to a polymer matrix with other degradation and swelling modes. Furthermore, all of the three fitting parameters were validated by the polymer characteristics, including polymer T_g, degradation rate constant, and the thickness increment rate constant. Generally, the new model applies for the drug release from polymer coatings with T_g in the vicinity of the drug release temperature, e.g. body temperature of 37 °C in this work. Applicability of the model beyond this range may be possible, but will certainly require experimental validation.

Acknowledgments

The authors are grateful for the financial support of this work by Boston Scientific Corporation. We would like to thank Prof. Mark D. Pagel at Case Western Reserve University for generously providing the usage of the HPLC.

Appendix A. Supplementary data

Supplementary data associated with this article can be found, in the online version, at doi:10.1016/j.jconrel.2009.04.016.

References

[1] B.L. van der Hoeven, N.M.M. Pires, H.M. Warda, P.V. Oemrawsingh, B.J.M. van Vlijmen, P.H.A. Quax, M.J. Schalij, E.E. van der Wall, J.W. Jukema, Drug-eluting stents: results, promises and problems, Int. J. Cardiol. 99 (2005) 9–17.
[2] L. Pinchuk, G.J. Wilson, J.J. Barry, R.T. Schoephoerster, J.-M. Parel, J.P. Kennedy, Medical applications of poly(styrene-block-isobutylene-block-styrene) ("SIBS"), Biomaterials 29 (2008) 448–460.
[3] R. Stein, FDA Panel Affirms Safety of New Artery Stents if Used Properly, December 8, 2006 available from http://www.washingtonpost.com/wp-dyn/content/article/2006/12/07/AR2006120700709.html.
[4] E. Grube, S. Silber, K.E. Hauptmann, R. Mueller, L. Buellesfeld, U. Gerckens, M.E. Russell, TAXUS I: six- and twelve-month results from a randomized, double-blind trial on a slow-release paclitaxel-eluting stent for de novo coronary lesions, Circulation 107 (2003) 38–42.
[5] M. Morice, P.W. Serruys, J.E. Sousa, J. Fajadet, E.B. Hayashi, M. Perin, A. Colombo, G. Schuler, P. Barragan, G. Guagliumi, F. Molnàr, R. Falotico, A randomized comparison of a sirolimus-eluting stent with a standard stent for coronary revascularization, New Engl. J. Med. 346 (2002) 1773–1780.
[6] M. Joner, A.V. Finn, A. Farb, E.K. Mont, F.D. Kolodgie, E. Ladich, R. Kutys, K. Skorija, H.K. Gold, R. Virmani, Pathology of drug-eluting stents in humans — delayed healing and late thrombotic risk, J. Am. Coll. Cardiol. 48 (2006) 193–202.
[7] T.F. Lüscher, J. Steffel, F.R. Eberli, M. Joner, G. Nakazawa, F.C. Tanner, R. Virmani, Drug-eluting stent and coronary thrombosis — biological mechanisms and clinical implications, Circulation 115 (2007) 1051–1058.
[8] S. Venkatraman, F. Boey, Release profiles in drug-eluting stents: issues and uncertainties, J. Control. Release 120 (2007) 149–160.
[9] R.A. Costa, A.J. Lansky, G.S. Mintz, R. Mehran, Y. Tsuchiya, M. Negoita, Y. Gilutz, E. Nikolsky, M. Fahy, R. Pop, E. Cristea, S. Carlier, G. Dangas, G.W. Stone, M.B. Leon, R. Muller, G. Techen, E. Grube, Angiographic results of the first human experience with everolimus-eluting stents for the treatment of coronary lesions (the FUTURE I trial), Am. J. Cardiol. 95 (2005) 113–116.
[10] S. Banai, S.D. Gertz, L. Gavish, M. Chorny, L.S. Perez, G. Lazarovichi, M. Ianculuvich, M. Hoffmann, M. Orlowski, G. Golomb, A. Levitzki, Tyrphostin AGL-2043 eluting stent reduces neointima formation in porcine coronary arteries, Cardiovasc. Res. 64 (2004) 165–171.
[11] E. Grube, L. Buellesfeld, BioMatrix (R) Biolimus A9 (R)-eluting coronary stent: a next-generation drug-eluting stent for coronary artery disease, Expert Rev. Med. Devices 3 (2006) 731–741.
[12] C.J. Pan, J.J. Tang, Y.J. Weng, J. Wang, N. Huang, Preparation, characterization and anticoagulation of curcumin-eluting controlled biodegradable coating stents, J. Control. Release 116 (2006) 42–49.
[13] F. Alexis, S.S. Venkatraman, S.K. Rath, F. Boey, In vitro study of release mechanisms of paclitaxel and rapamycin from drug-incorporated biodegradable stent matrices, J. Control. Release 98 (2004) 67–74.
[14] R. Wessely, A. Kastrati, J. Mehilli, A. Dibra, J. Pache, A. Schömig, Randomized trial of rapamycin- and paclitaxel-eluting stents with identical biodegradable polymeric coating and design, Eur. Heart J. 28 (2007) 2720–2725.
[15] L.L. Lao, S.S. Venkatraman, Adjustable paclitaxel release kinetics and its efficacy to inhibit smooth muscle cells proliferation, J. Control. Release 130 (2008) 9–14.
[16] U. Westedt, M. Wittmar, M. Hellwig, P. Hanefeld, A. Greiner, A.K. Schaper, T. Kissel, Paclitaxel releasing films consisting of poly(vinyl alcohol)-graft-poly(lactide-co-glycolide) and their potential as biodegradable stent coatings, J. Control. Release 111 (2006) 235–246.
[17] P. Hanefeld, U. Westedt, R. Wombacher, T. Kissel, A. Schaper, J.H. Wendorff, A. Greiner, Coating of poly(p-xylylene) by PLA–PEO–PLA triblock copolymers with excellent polymer–polymer adhesion for stent applications, Biomacromolecules 7 (2006) 2086–2090.
[18] B. Balakrishnan, J.F. Dooley, G. Kopia, E.R. Edelman, Intravascular drug release kinetics dictate arterial drug deposition, retention, and distribution, J. Control. Release 123 (2007) 100–108.
[19] B. Balakrishnan, J. Dooley, G. Kopia, E.R. Edelman, Thrombus causes fluctuations in arterial drug delivery from intravascular stents, J. Control. Release 131 (2008) 173–180.
[20] V.B. Kolachalama, A.R. Tzafriri, D.Y. Arifin, E.R. Edelman, Luminal flow patterns dictate arterial drug deposition in stent-based delivery, J. Control. Release 133 (2009) 24–30.
[21] P.T. Mather, Q. Ge, C. Liu, Shape memory polymers based on semicrystalline thermoplastic polyurethanes bearing nanostructured hard segments, U.S. Patent 7,091,297 B2, August 15, 2006.
[22] P.T. Knight, K.-M. Lee, H. Qin, P.T. Mather, Biodegradable thermoplastic polyurethanes incorporating polyhedral oligosilsesquioxane, Biomacromolecules 9 (2008) 2458–2467.
[23] G.Z. Li, L.C. Wang, H.L. Ni, C.U. Pittman, Polyhedral oligomeric silsesquioxane (POSS) polymers and copolymers: a review, J. Inorg. Organomet. Polym. 11 (2001) 123–154.
[24] J. Siepmann, N.A. Peppas, Modeling of drug release from delivery systems based on hydroxypropyl methylcellulose (HPMC), Adv. Drug Deliv. Rev. 48 (2001) 139–157.
[25] J. Siepmann, A. Göpferich, Mathematical modeling of bioerodible, polymeric drug delivery systems, Adv. Drug Deliv. Rev. 48 (2001) 229–247.
[26] J. Crank, Diffusion in a plane sheet, The Mathematics of Diffusion, 2nd ed., Oxford University Press, London, 1975, pp. 47–49.
[27] M.P. Mullarney, T.A.P. Seery, R.A. Weiss, Drug diffusion in hydrophobically modified N,N-dimethylacrylamide hydrogels, Polymer 47 (2006) 3845–3855.
[28] D.Y. Arifin, L.Y. Lee, C.-H. Wang, Mathematical modeling and simulation of drug release from microspheres: implications to drug delivery systems, Adv. Drug Deliv. Rev. 58 (2006) 1274–1325.
[29] W. Weibull, A statistical distribution function of wide applicability, J. Appl. Mech. 18 (1951) 293–297.
[30] F. Langenbucher, Linearization of dissolution rate curves by the Weibull distribution, J. Pharm. Pharmacol. 24 (1972) 979–981.
[31] J.N. Etters, Diffusion equation made easy, Text. Chem. Color. 12 (1980) 140–145.
[32] P. Costa, J. Manuel, S. Lobo, Modeling and comparison of dissolution profiles, Eur. J. Pharm. Sci. 13 (2001) 123–133.

[33] P.V. Pedersen, J.W. Myrick, Versatile kinetic approach to analysis of dissolution data, J. Pharm. Sci. 67 (1978) 1450–1455.
[34] F.N. Christensen, F.Y. Hansen, H. Bechgaard, Physical interpretation of parameters in the Rosin–Rammler–Sperling–Weibull distribution for drug release from controlled release dosage forms, J. Pharm. Pharmacol. 32 (1980) 580–582.
[35] S.K. Dordunoo, H.M. Burt, Solubility and stability of taxol: effects of buffers and cyclodextrins, Int. J. Pharm. 133 (1996) 191–201.
[36] K.J. Volk, S.E. Hill, E.H. Kerns, M.S. Lee, Profiling degradants of paclitaxel using liquid chromatography mass spectrometry and liquid chromatography-tandem mass spectrometry substructural techniques, J. Chromatogr. B 696 (1997) 99–115.
[37] K. Elkharraz, N. Faisant, C. Guse, F. Siepmann, B. Arica-Yegin, J.M. Oger, R. Gust, A. Goepferich, J.P. Benoit, J. Siepmann, Paclitaxel-loaded microparticles and implants for the treatment of brain cancer: preparation and physicochemical characterization, Int. J. Pharm. 314 (2006) 127–136.
[38] N. Baek, J. Lee, K. Park, Aqueous N,N-diethylnicotinamide (DENA) solution as a medium for accelerated release study of paclitaxel, J. Biomater. Sci., Polym. Ed. 15 (2004) 527–542.
[39] P.L. Ritger, N.A. Peppas, A simple equation for description of solute release I. Fickian and non-Fickian release from non-swellable devices in the form of slabs, spheres, cylinders or discs, J. Control. Release 5 (1987) 23–36.
[40] A. Charlier, B. Leclerc, G. Couarraze, Release of mifepristone from biodegradable matrices: experimental and theoretical evaluations, Int. J. Pharm. 200 (2000) 115–120.
[41] S. Yoshioka, Y. Aso, S. Kojima, Drug release from poly(DL-lactide) microspheres controlled by gamma-irradiation, J. Control. Release 37 (1995) 263–267.
[42] M.O. Omelczuk, J.W. McGinity, The influence of polymer glass-transition temperature and molecular-weight on drug release from tablets containing poly (DL-lactic acid), Pharm. Res. 9 (1992) 26–32.
[43] D. Ehlich, H. Sillescu, Tracer diffusion at the glass transition, Macromolecules 23 (1990) 1600–1610.
[44] D.D. Deppe, A. Dhinojwala, J.M. Torkelson, Small molecule probe diffusion in thin polymer films near the glass transition: a novel approach using fluorescence nonradiative energy transfer, Macromolecules 29 (1996) 3898–3908.
[45] T. Kokubo, K. Sugibayashi, Y. Morimoto, Interaction between drugs and pressure-sensitive adhesives in transdermal therapeutic systems, Pharm. Res. 11 (1994) 104–107.
[46] J.S. Vrentas, J.L. Duda, H.-C. Ling, Free-volume theories for self-diffusion in polymer–solvent systems. I. Conceptual differences in theories, J. Polym. Sci., Polym. Phys. Ed. 23 (1985) 275–288.
[47] J.S. Vrentas, J.L. Duda, H.-C. Ling, A.-C. Hou, Free-volume theories for self-diffusion in polymer–solvent systems. II. Predictive capabilities, J. Polym. Sci., Polym. Phys. Ed. 23 (1985) 289–304.
[48] J.M. Zielinski, J.L. Duda, Predicting polymer/solvent diffusion coefficients using free-volume theory, AlChE J. 38 (1992) 405–415.
[49] M.L. Williams, R.F. Landel, J.D. Ferry, The temperature dependence of relaxation mechanisms in amorphous polymers and other glass-forming liquids, J. Am. Chem. Soc. 77 (1955) 3701–3707.